The effect of non-local electron scattering on the current-perpendicular-to-plane-mode magnetoresistance of magnetic multilayers

2000 J. Phys.: Condens. Matter 12 4263

(http://iopscience.iop.org/0953-8984/12/18/311)

J. Phys.: Condens. Matter **12** (2000) 4263–4276. Printed in the UK PII: S0953-8984(00)08053-X

The effect of non-local electron scattering on the current-perpendicular-to-plane-mode magnetoresistance of magnetic multilayers

D Bozec†, M J Walker†, M A Howson†, B J Hickey†, S Shatz‡ and N Wiser‡

† Department of Physics and Astronomy, E C Stoner Laboratory, University of Leeds, Leeds LS2 9JT, UK

‡ Jack and Pearl Resnick Institute for Advanced Technology, Department of Physics, Bar-Ilan University, Ramat-Gan, Israel

Received 22 September 1999, in final form 10 February 2000

Abstract. We have carried out an experimental and theoretical study of non-local electron scattering in magnetic multilayers by measuring the magnetoresistance MR(H) in the CPP (current-perpendicular-to-plane) mode for two samples consisting of different magnetic layers (M1, M2) separated by non-magnetic layers (NM). For the two samples, the ordering of the layers was as follows: $[M1/NM/M2/NM]_N$ and $[M1/NM]_N[M2/NM]_N$. If the non-local character of the electron scattering were unimportant, the two samples would yield identical curves for MR(H) in the CPP mode. However, our measured MR(H) curves are completely different for the two samples. This demonstrates the importance of non-local electron scattering. For our measurements, M1 = Fe(50 Å), M2 = Co(20 Å), NM = Cu(200 Å) for Fe–Co samples, and M1 = Co(10 Å), M2 = Co(60 Å), NM = Cu(200 Å) for the Co–Co samples. To confirm our ideas, we calculated MR(H), including the effect of non-local electron scattering, and obtained quantitative agreement with experiment.

1. Introduction

The giant magnetoresistance exhibited by magnetic multilayers continues to be an area of considerable experimental and theoretical activity [1]. Recently, there has been great interest in the measurement of the magnetoresistance MR(H) measured in the CPP mode—that is, with the current perpendicular to the plane of the layers (for recent reviews, see [2, 3]). Although measurements of MR(H) are technically easier to perform in the CIP mode (current parallel to the plane of the layers), there are important advantages to measurements in the CPP mode. For example, CPP MR(H) data yield information about the spin diffusion length [4, 5]. The importance of this parameter for determining MR(H) is not limited to magnetic multilayers. For granular systems as well, it was recently shown [6] that the spin diffusion length influences the values of MR(H).

In this paper, we investigate, both experimentally and theoretically, the role played by non-local electron scattering for determining the magnetic field dependence of the CPP MR(H). Our principal result is that for certain samples, the important length scale is the electron mean free path, rather than the spin diffusion length.

As is well known, the giant magnetoresistance (GMR) occurs in magnetic multilayers because the rate of electron scattering depends of the direction of the electron spin. If the electron does not flip its spin upon scattering, then the spin-up electrons and the spin-down

0953-8984/00/184263+14$30.00

electrons constitute two separate currents, experiencing different resistances, as if they were flowing in two separate parallel wires. The resistance of magnetic multilayers is often analysed in terms of the series resistor model [4], which predicts that for each of the two currents, the resistances of the different layers will add in series in the CPP mode, because each electron will pass through all the layers. Therefore, it would seem that in the absence of spin flipping, two magnetic multilayers that differ only in the ordering of the layers would yield identical CPP MR(H) curves.

This idea has been tested by Pratt and co-workers at Michigan State University, who measured [7] the CPP MR(H) for the two configurations $[\mathrm{Py/Cu/Co/Cu}]_N$ and $[\mathrm{Py/Cu}]_N[\mathrm{Co/Cu}]_N$ (denoted as 'interleaved' and 'separated' configurations, respectively), where Py is $Ni_{84}Fe_{16}$. Since the interleaved and separated configurations differ *only* in the ordering of the layers, the series resistor model predicts identical MR(H) curves for the two configurations. However, the MSU group found [7] that the two resulting MR(H) curves were completely different. They attributed this unexpected result to the short spin diffusion length in Py, implying mixing between the spin-up and spin-down electron currents.

We here explore this question further by measuring the CPP MR(H) for magnetic multilayers consisting of magnetic metals that are *not* expected to have a short spin diffusion length. A particularly attractive choice is Co, whose spin diffusion length has been measured, yielding values of 450 Å [8,9] and 1000 Å [9], which are of course very much larger than the thickness of the Co layers. In our first set of samples, the second magnetic metal was Fe, whose spin diffusion length is not known although it is certainly longer than that in Py. To ensure that a short spin diffusion length would not be the explanation for our data, we repeated the measurements of the CPP MR(H) using Co for *both* magnetic layers. We obtained magnetic layers with *different* coercivities by using Co layers of two different thicknesses, one being Co(10 Å) and the other being Co(60 Å).

Our principal result is that in all cases, the MR(H) curves are very different when measured for the interleaved and for the separated configurations. This is true regardless of which combination of magnetic metals is used. Since we obtained this result for magnetic metals having a long spin diffusion length, it follows that spin flipping is *not* the explanation for the marked differences between the MR(H) curves for the separated an interleaved configurations.

In this paper, we propose a different explanation for the dependence of the MR(H) curves on the ordering of the layers. Our proposal is confirmed by calculations that yield quantitative agreement with the MR(H) data. The idea is that the (non-spin-flipping) electron mean free path is long enough that the electron 'feels' *pairs* of neighbouring magnetic layers. As a result, individual layers do *not* determine the scattering potential, and the series resistor model does not apply. Rather, the scattering potential is due to the relative orientation of the magnetic moments in *pairs* of neighbouring magnetic layers. Since the scattering is not due to the properties of a *single* magnetic layer, this effect may be termed 'non-local' scattering.

It should be mentioned that even though the electron mean free path is far longer than the thickness of the magnetic layers, one need consider *only* nearest-neighbour magnetic layers. The reason is that the structure of the interleaved configuration repeats itself after each pair of nearest-neighbour magnetic layers. In other words, Fe/Cu/Co/Cu forms the 'unit cell' for this periodic structure. As in the case for any periodic structure, there is no need to consider additional 'unit cells' when writing the scattering potential, since they would not change the calculated resistivity.

For the situation described above, the contribution of an electron scattering event to the spin-dependent resistance depends [10] on the cosine of the angle θ_{ij} between the moments of neighbouring magnetic layers, denoted as i and j. Since θ_{ij} is very different for the interleaved and separated configurations, there is no reason to expect the MR(H) curves to be identical for

the two configurations. These ideas formed the basis of a detailed calculation of the MR(H). The agreement we obtain between our calculated and measured values lends important support to our interpretation of the MR(H) data.

In section 2, we describe the samples and give some experimental details. In section 3, the data are presented; this is followed by a qualitative explanation of the data in section 4 and a quantitative calculation in section 5. Conclusions are presented in section 6.

2. Experimental details and description of the samples

The multilayers were grown on sapphire ($11\bar{2}0$) substrates by molecular beam epitaxy in our VG-80M MBE facility, with a base pressure of typically 4×10^{-11} mbar. The ultra-high-vacuum system contained a Knudsen cell for the deposition of Cu and electrons guns for the deposition of Fe, Co, and Nb. Our CPP measurements used the superconducting Nb electrode technique, as developed by Pratt *et al* [11]. The CPP samples are sandwiched between strips of Nb 1 mm wide. The superconducting equipotential [12, 13] ensures that the current is perpendicular to the layers. The sapphire substrate was heated up to 950 °C to clean the surface and allow epitaxial growth of the Nb in the (110) direction. A Nb strip of thickness 1500 Å was first deposited at a growth rate of 1 Å s^{-1}. Then, 30 Å of Cu was deposited at 375 °C as a buffer layer, to seed the growth in the (111) direction. The system was then cooled to room temperature to allow the deposition of the multilayer. The evaporation rates for the Co, Fe, and Cu were all 1 Å s^{-1}. Finally, a strip of Nb, of thickness 1500 Å, was grown on top of the multilayer. The CPP geometry was maintained by evaporating through several masks cut into a single piece of stainless steel, which was repositioned several times during the growth cycle.

We used a SQUID-based current comparator, working at 0.1% precision, to measure changes in the sample resistance of order 10 pΩ. To avoid driving the Nb normal, the CPP measurements were performed at 4.2 K in magnetic fields below 3 kOe. Consistency between the interleaved and separated samples was enhanced by growing the two configurations during the same run for each value of N.

For the samples using Fe and Co as the two magnetic metals, the thickness of the layers was 50 Å for Fe and 20 Å for Co, which gives a difference of 700 Oe in the coercive fields of the two metals. For the samples using Co for both ferromagnetic layers, the thicknesses of the Co layers were 10 Å and 60 Å, yielding a difference of nearly 1000 Oe in the coercive fields. The thickness of the non-magnetic layers of Cu was always 200 Å, a value large enough to ensure magnetic decoupling between the ferromagnetic layers for both dipolar and exchange interactions [11, 14].

3. Measured data

3.1. The Fe–Co samples

Our measurements of the CPP MR(H) were carried out on the interleaved configuration [Fe(50 Å)/Cu(200 Å)/Co(20 Å)/Cu(200 Å)]$_N$ and also on the separated configuration [Fe(50 Å)/Cu(200 Å)]$_N$[Co(20 Å)/Cu(200 Å)]$_N$ for $N = 2, 4, 8$, where N is the number of repeats. The data are presented for the three values of N in figures 1(a)–1(c), where the circles and squares represent the measured values for the separated and interleaved configurations, respectively.

There are several characteristic features of these data, all of which can be explained in terms of non-local electron scattering:

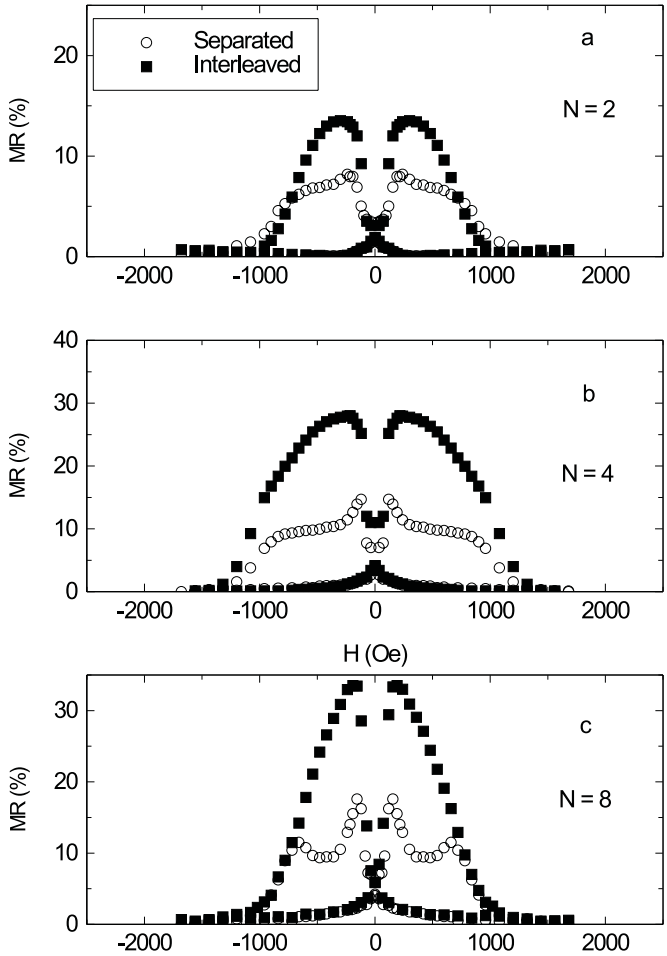

Figure 1. Magnetoresistance MR(H) for the interleaved (squares) and separated (circles) Fe–Co samples for the indicated number of repeats.

(i) The most important feature is certainly the striking difference between the MR(H) curves for the two configurations, both in shape and in magnitude.
(ii) For each N, the maximum value of MR(H) is larger for the interleaved configuration.
(iii) The MR(H) curve for the interleaved configuration exhibits a single peak, whereas for the separated configuration, MR(H) is the superposition of two peaks. For small N (=2, 4), the second peak is much broader and much less delineated than the first. However, for $N = 8$, the second peak in MR(H) is clearly visible.

3.2. The Co–Co samples

Our measurements of the CPP MR(H) were carried out on the interleaved configuration [Co(10 Å)/Cu(200 Å)/Co(60 Å)/Cu(200 Å)]$_N$ and also on the separated configuration [Co(10 Å)/Cu(200 Å)]$_N$ [Co(60 Å)/Cu(200 Å)]$_N$ for $N = 4$, 6, 8. The data are presented for the three values of N in figures 2(a)–2(c), where the circles and squares represent the measured values for the separated and interleaved configurations, respectively.

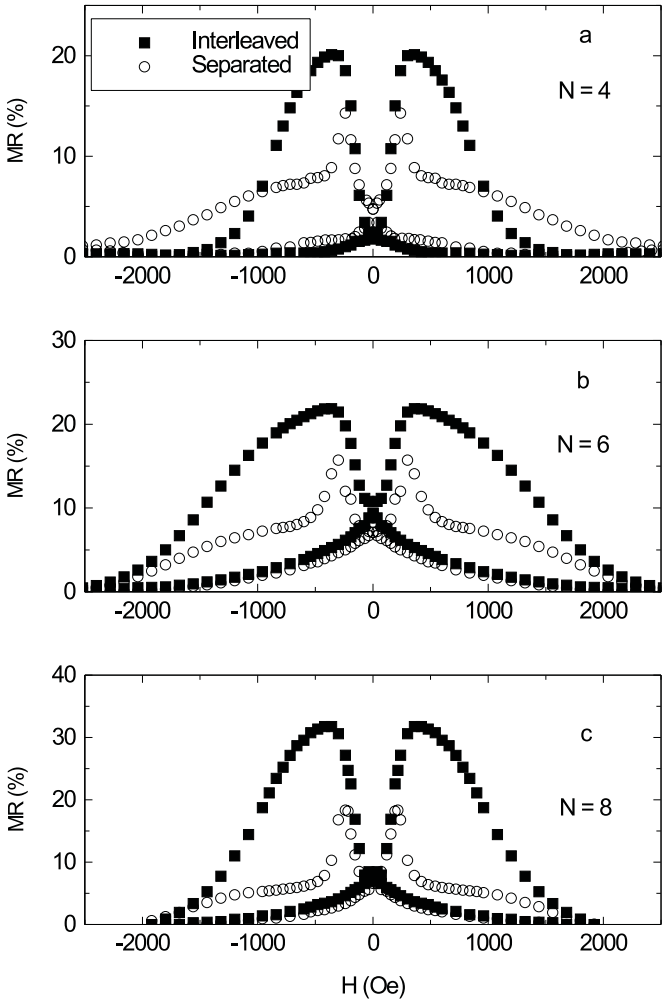

Figure 2. Magnetoresistance MR(H) for interleaved (squares) and separated (open circles) Co–Co samples for the indicated number of repeats.

We see that these data for the Co–Co multilayers share the same features as those listed above for the Fe–Co multilayers. The only exception is that for the Co–Co samples, the separated configuration does not yield two distinct peaks for MR(H) even for $N = 8$.

3.3. Magnetization

To ensure that the differing results for MR(H) for the two configurations are not due to differences in their magnetic properties, the magnetization of each sample was measured. The magnetization loops were isotropic in the plane of the layers. The magnetization data for $N = 8$, normalized to the saturation magnetization, are plotted in figure 3. The initial sharp rise of the curve is due to the magnetization of the thicker Co(60 Å) layers, followed by the more modest increase of the curve as the thinner Co(10 Å) layers also approach saturation at much larger fields. Of particular interest for the MR(H) curves in the separated configuration

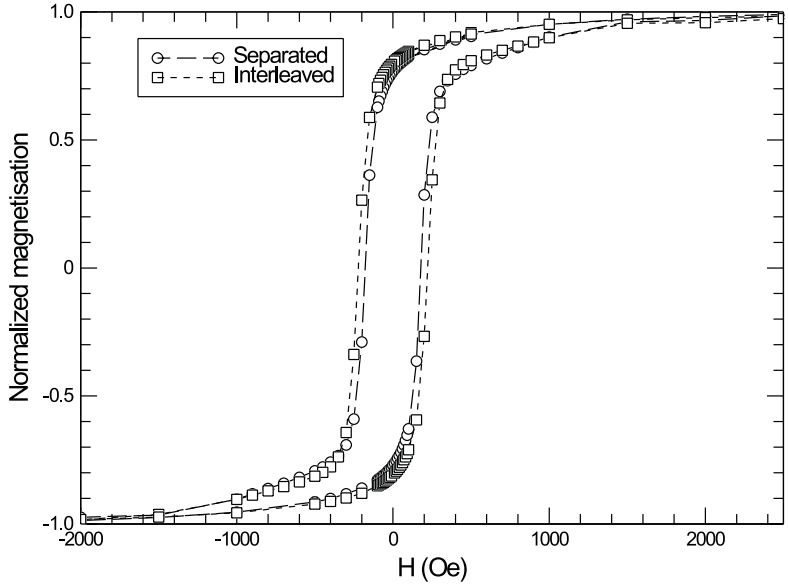

Figure 3. Comparison of the magnetization curves for interleaved (open squares) and separated (open circles) Co–Co samples for $N = 8$, measured at 12 K.

is the fact that the coercive field (dominated by the thicker Co(60 Å) layers) occurs at about 180 Oe.

As seen in the figure, the two configurations yield the same field dependence for the magnetization. This confirms that the magnetic layers are uncoupled and become magnetized independently.

4. Qualitative explanation

Kinetic theory arguments, confirmed by recent measurements [15] of the GMR as a function of the number of repeats, show that the electron mean free path is far longer than the thicknesses of the magnetic layers. Therefore, the potential 'felt' by the electron is the combined potential of a neighbouring pair of magnetic layers. This may be termed 'non-local' electron scattering, because a property of *pairs* of neighbouring layers determines the resistivity. The contribution of the spin-dependent resistivity depends on the cosine of the angle θ_{ij} between moments of neighbouring i, j magnetic layers [10]. This is the key to understanding the data.

For the interleaved configuration, neighbouring magnetic layers are *different*, and hence the maximum angle θ_{ij} is *large*, whereas in the separated configuration, neighbouring magnetic layers are the *same* (except for the boundary layer), and hence the angle θ_{ij} is *small*. Since $\mathrm{MR}(H)$ depends on this angle, there is no reason to expect $\mathrm{MR}(H)$ to be the same for the two configurations. This explains the first feature of the data mentioned above.

From the above considerations, it follows immediately that $\mathrm{MR}(H)$ will be larger for interleaved multilayers than for separated multilayers, because the angle θ_{ij} is larger for the former configuration. This explains the second feature of the data mentioned above.

For the interleaved configuration, there is only *one* angle θ_{ij} that is relevant, namely, the angle between the moments of *different* neighbouring magnetic layers. Therefore, there will be only *one* peak, as the angle θ_{ij} becomes progressively larger, passes through a maximum

at the first type of magnetic layers saturate, and then becomes smaller as the second type of magnetic layers also saturate.

For the separated configuration, there are *two* angles that are relevant (in addition to a single boundary layer, which will be discussed presently), namely, the angle between each of the *two* different sets of neighbouring magnetic layers. As each of these two angles passes through its maximum, a peak is obtained for MR(H). The MR(H) curve thus consists of *two* overlapping peaks, with each maximum occurring at the value of the magnetic field that corresponds to the appropriate coercive field. This explains the third feature of the data mentioned above.

In figure 4, we compare the field dependence of the magnetoresistance for the separated configuration with that of the magnetization, beginning from remanence. We note that the peak of MR(H) occurs precisely at the coercive field of the magnetization curve (about 180 Oe). This is an important prediction of our analysis. Moreover, the saturation field of the magnetization curve corresponds closely to the saturation field of the MR(H) curve, as expected.

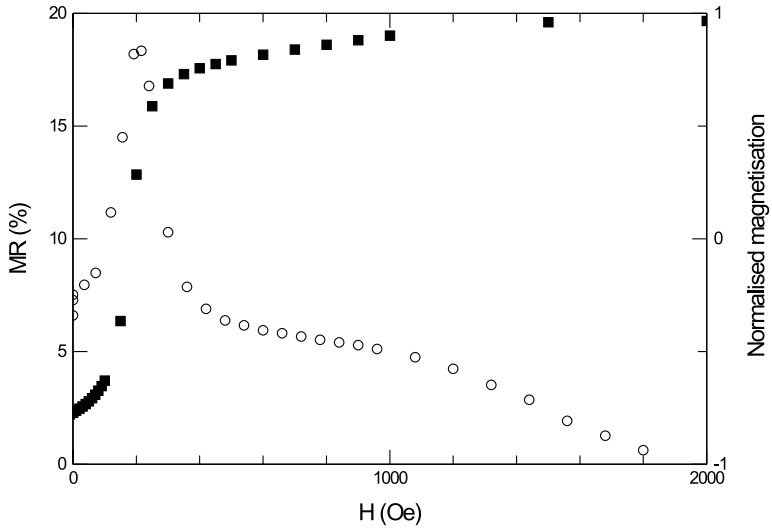

Figure 4. Comparison between the field dependence of the magnetization from remanence to saturation (solid squares) and of the magnetoresistance (open circles) for Co–Co samples for $N = 8$ for the separated configuration.

5. Calculations

The above ideas can be made quantitative. According to the phenomenological theory of Wiser [16], for the geometry under consideration here (moments are first saturated into a parallel state; then the field is applied in the opposite direction, causing an increase in the angle between neighbouring moments), the contribution to the magnetoresistance due to an ij-pair of neighbouring magnetic layers is

$$\mathrm{MR}_{ij}(H) = c_{ij}(1 - \cos\theta_{ij}(H))^2. \tag{1}$$

For our samples, there are three parameters c_{ij} corresponding to the three types of neighbouring pairs of magnetic layers: $i = j = 1; i = j = 2; i = 1, j = 2$, where 1 and 2 refer to the two different magnetic layers. The interleaved configuration has only $i = 1, j = 2$ neighbours, whereas the separated configuration contains all three types. For a

sample containing N repeats, the separated configuration consists of $N-1$ pairs of $i=j=1$ neighbours, followed by one pair of $i=1$, $j=2$ neighbours (the boundary layer), and then followed by $N-1$ pairs of $i=j=2$ neighbours. For each value of N, the parameters c_{ij} were determined by fitting to the MR(H) data.

We shall now establish the magnetic field dependence of the angle $\theta_{ij}(H)$.

5.1. The interleaved configuration

Consider first the interleaved configuration. The magnetization increases linearly with field (except near saturation, where it increases more slowly). Since the magnetization is proportional to the cosine of the angle between the magnetic moment and the field, it follows that for the two layers, $\cos\theta_1$ and $\cos\theta_2$ are each linear in the field, but with different coefficients, increasing from -1 to $+1$ as the magnetic field increases from zero to saturation. Equation (1) contains $\cos\theta_{1,2}=\cos(\theta_1-\theta_2)$. Expanding $\cos(\theta_1-\theta_2)$ in terms of $\cos\theta_1$ and $\cos\theta_2$ gives the required field dependence.

The maximum value of $\theta_{1,2}$ is usually quite large, as can readily be seen. Say, for example, that the saturation magnetic field for the second type of magnetic layer, $H_{sat,2}$, is three times larger than that for the first type of magnetic layer, $H_{sat,1}$. Then, as the field increases up to $H_{sat,1}$, the angle θ_1 increases to 180°, while the angle θ_2 increases only to 60°. Therefore, at $H_{sat,1}$, the value of $\theta_{1,2}$ is 120°. For $H > H_{sat,1}$, the magnitude of θ_1 remains 180°, while the angle θ_2 continues to increase. Thus, as H increases beyond $H_{sat,1}$, the magnitude of $\theta_{1,2}$ decreases from 120°, eventually reaching zero when H reaches $H_{sat,2}$.

Near saturation, the expressions for $\cos\theta_1$ and $\cos\theta_2$ must be modified to take into account that the magnetization approaches saturation more slowly than linearly. If this is not taken into account, the calculated peak in MR(H) would be sharper than the data show. The reason is that for a linear dependence, the angle $\theta_{1,2}$ changes abruptly from increasing with magnetic field (for $H < H_{sat,1}$) to decreasing with magnetic field (for $H > H_{sat,1}$). To avoid this unphysical behaviour, we modelled the field dependence of the magnetization by a tanh function near saturation. The tanh function is qualitatively similar to the measured approach to saturation for the magnetization. The value of the magnetic field at which the tanh function smoothly joins the linear function was taken as an adjustable parameter.

The calculated results for MR(H) for the Fe–Co samples in the interleaved configuration, together with the data, are presented in figures 5(a)–5(c) for three values of N. The corresponding calculated results for MR(H) for the Co–Co samples, together with the data, are presented in figures 6(a)–6(c). For each set of samples, the agreement between the calculated curves and the data is evident from the figures.

5.2. The separated configuration

We now consider the separated configuration. If the magnetic layers were ideal single-domain structures, then the magnetic moment of each magnetic layer would react identically to the magnetic field and the angles $\theta_{1,1}$ and $\theta_{2,2}$ would both be zero at all fields. However, because of the presence of domains and of structural imperfections in the Co layers, each layer reverses its magnetization at a somewhat different rate. As a result, the angles $\theta_{1,1}$ and $\theta_{2,2}$ become non-zero as the field is increased, pass through a maximum at the coercive field, and then decrease to zero as saturation is approached. We assumed a simple parabolic form for each of the two angles $\theta_{1,1}$ and $\theta_{2,2}$ with the maximum value of each parabola taken as an adjustable parameter for each value of N. In practice, the maximum angles $\theta_{max,1,1}$ and $\theta_{max,2,2}$ cannot be determined by fitting to the MR(H) data for the following reason. Because these angles

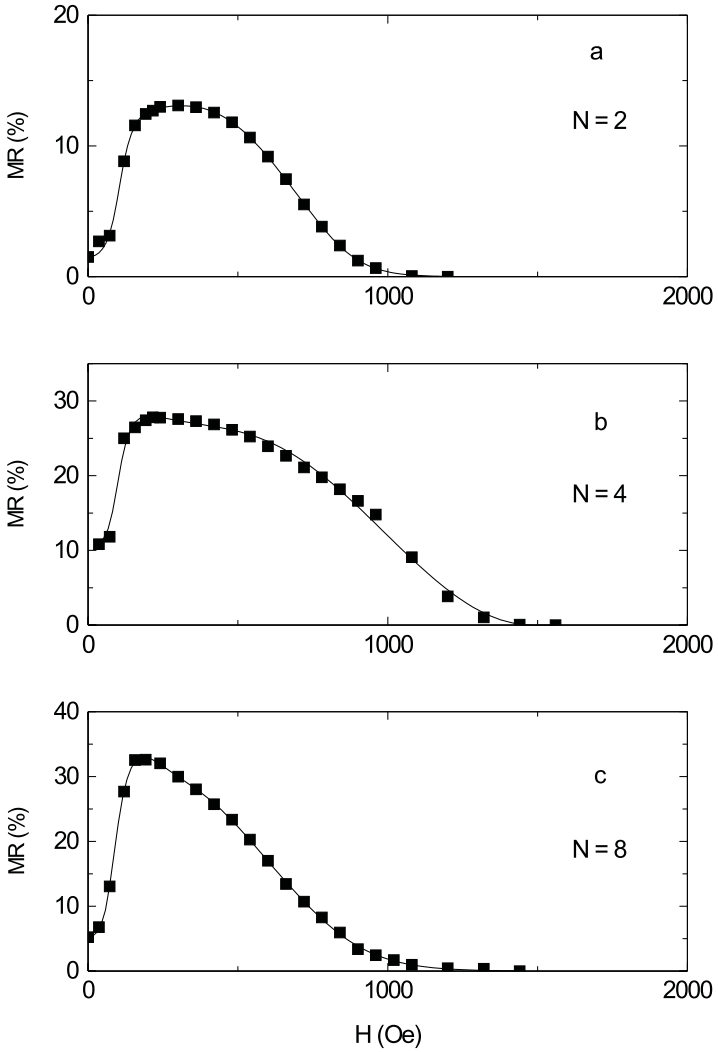

Figure 5. Comparison between the calculated curves (solid lines) and the data points (squares) for MR(H) for the interleaved Fe–Co samples for the indicated number of repeats.

are small, equation (1) can be expanded to yield

$$\mathrm{MR}_{ii} = c_{ii}\left(\frac{1}{2}\theta_{ii}^2\right)^2 \propto c_{ii}(\theta_{max,ii})^4 \tag{2}$$

and this *combination* of c_{ii} and $\theta_{max,ii}$ serves as a *single* fitting parameter. Nevertheless, some numerical tests that we have carried out suggest that both $\theta_{max,1,1}$ and $\theta_{max,2,2}$ lie in the range of 15°–30°. These values are, of course, much smaller than the maximum value of the angle $\theta_{1,2}$. This explains why MR(H) is larger for the interleaved configuration than for the separated configuration.

The calculated results for MR(H) for the Fe–Co samples in the separated configuration, together with the data, are presented in figures 7(a)–7(c) for three values of N. The corresponding calculated results for MR(H) for the Co–Co samples, together with the data, are

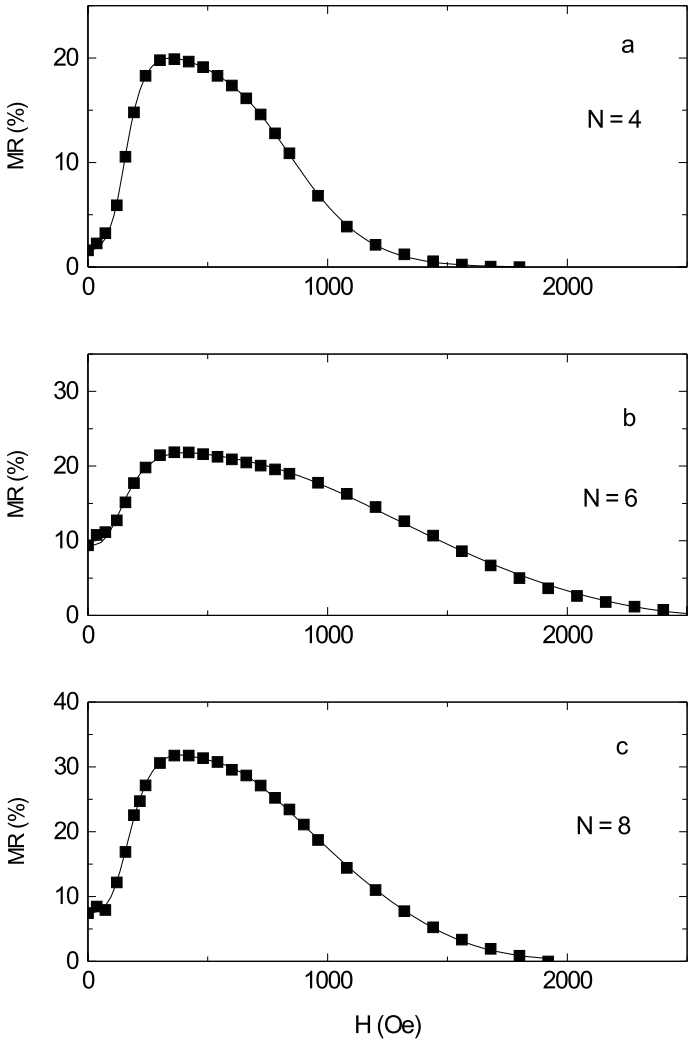

Figure 6. Comparison between the calculated curves (solid lines) and the data points (squares) for MR(H) for the interleaved Co–Co samples for the indicated number of repeats.

presented in figures 8(a)–8(c). For each set of samples, the agreement between the calculated curves and the data is evident from the figures.

5.3. The boundary layer

The boundary layer for the separated configuration merits a separate discussion. One might think that for N as large as 8, the boundary layer is not important, being only one pair of neighbouring layers, as compared to 15 other (non-boundary) pairs of neighbours. However, such an assessment would be in error. Indeed, it is precisely the effect of the boundary layer than causes the second peak to become indistinct in the MR(H) curves.

The importance of the contribution of the boundary layer to MR(H) is twofold: both its magnitude and the position of its peak. The large magnitude of the contribution to $\mathrm{MR}_{ij}(H)$

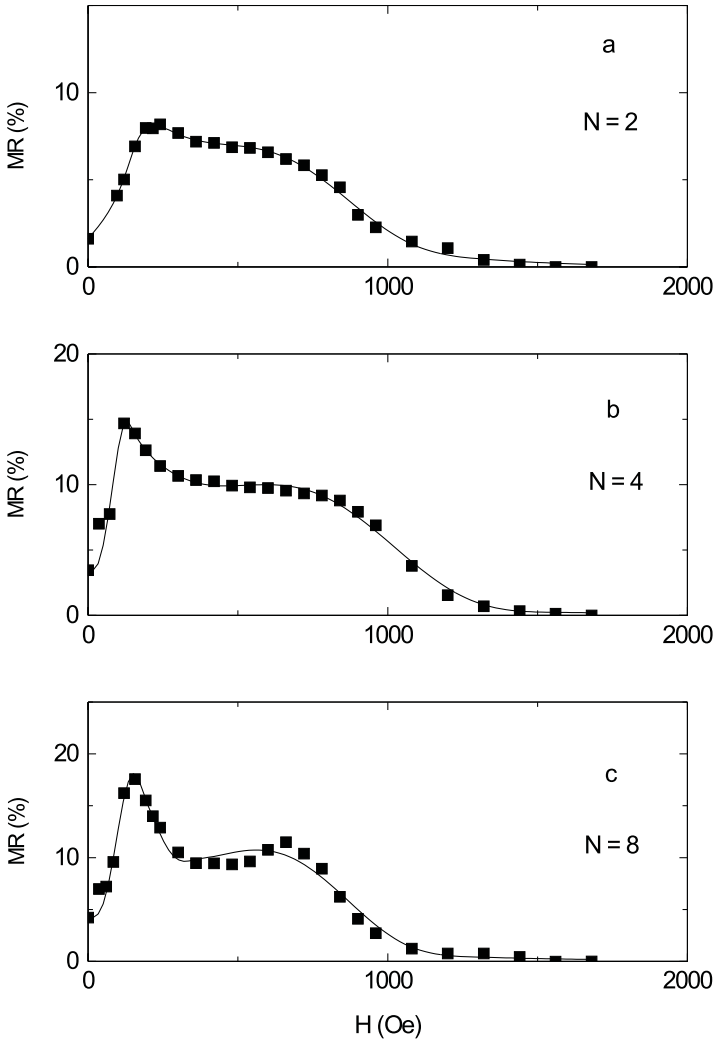

Figure 7. Comparison between the calculated curves (solid lines) and the data points (squares) for MR(H) for the separated Fe–Co samples for the indicated number of repeats.

due to the boundary layer stems from the much larger value of its angle $\theta_{1,2}$. But there is also another reason for the importance of the boundary layer, related to the *position* of its peak contribution to MR(H). In the separated configuration, the 'valley' between the two peaks occurs at the saturation field of the first type of magnetic layer. But this is precisely the position of the *peak* of the contribution of the boundary layer, as explained in the discussion of the interleaved configuration. (The boundary layer is essentially an 'interleaved' pair of neighbours embedded within the separated configuration.)

To illustrate these points, we plot in figure 9 the calculated results for the Co–Co sample having $N = 8$. The solid curve represents MR(H), as given in figure 8(c). The dashed curve is the contribution due to the boundary layer, and the dot–dash curve gives MR(H) *without* the contribution of the boundary layer (the sum of the dashed and dot–dash curves equals the solid curve). It is seen that the dot–dash curve consists of two distinct peaks, as expected. However,

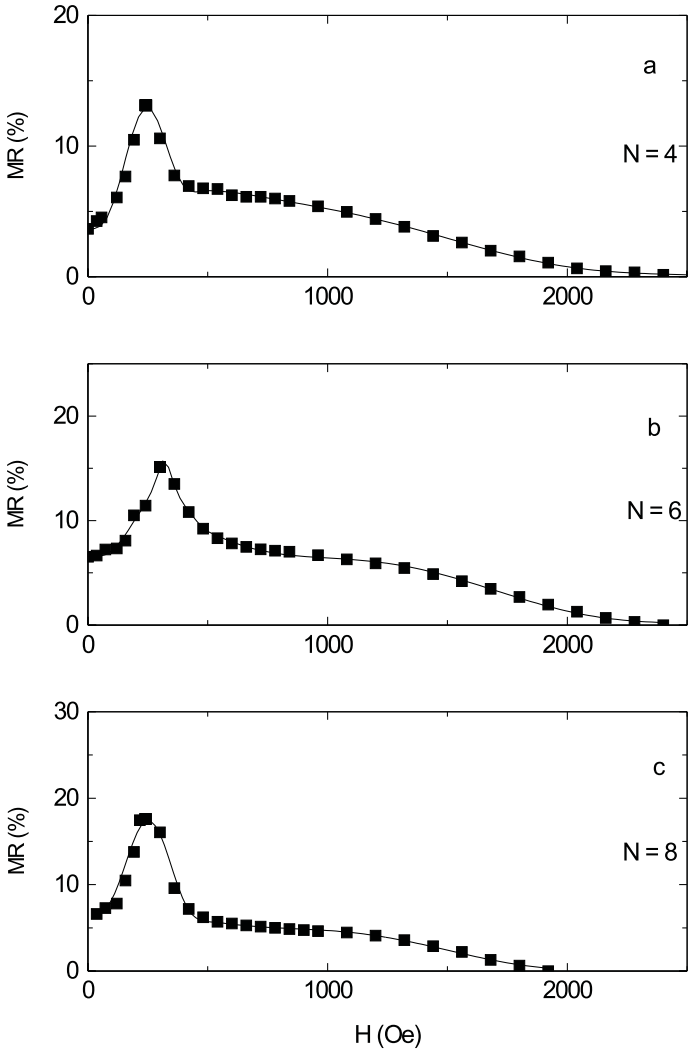

Figure 8. Comparison between the calculated curves (solid lines) and the data points (squares) for MR(H) for the separated Co–Co samples for the indicated number of repeats.

the second peak is washed out by the dashed curve, whose maximum occurs precisely in the 'valley' between the two peaks in the dot–dash curve. We also note the magnitude of the dashed curve. The single boundary layer makes a contribution to MR(H) as large as the second peak due to *all seven* ($N - 1$) other pairs of neighbours. This is the reason that the second peak is washed out.

6. Conclusions

We have shown, both experimentally and theoretically, that the series resistor model is not appropriate to describe the magnetoresistance of magnetic multilayers, measured in the CPP mode, for which the mean free path is longer than the bilayer thickness. In particular, the

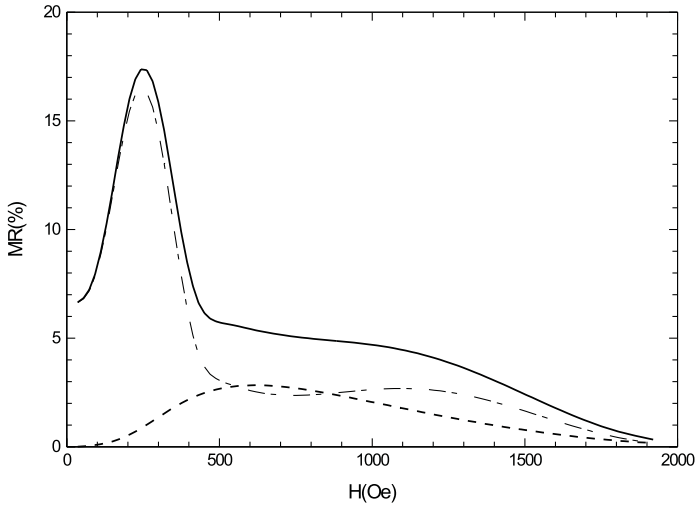

Figure 9. Calculated MR(H) (solid curves) for the Co (10 Å) and Co(60 Å) sample for $N = 8$ in the separated configuration. The dashed curve gives the contribution due the boundary layer, and the dot–dash curve gives MR(H) without the boundary layer.

values obtained for the CPP MR(H) depend very significantly on the ordering of the magnetic layers, in contrast to the prediction of the series resistor model. This model is appropriate only for magnetic multilayers for which the non-spin-flip electron mean free path is so short that the electron does not reach the neighbouring magnetic layer between scattering events.

Acknowledgments

It is a pleasure to acknowledge support from the UK–Israel Science and Technology Research Fund and the UK EPSRC. D Bozec thanks the University of Leeds for financial support, and he also thanks Professor W P Pratt Jr for his hospitality at Michigan State University where the magnetization measurements were performed.

References

[1] Baibich M N, Broto J M, Fert A, Vandau F N, Petroff F and Etienne P 1988 *Phys. Rev. Lett.* **61** 2472
Parkin S S P 1993 *Phys. Rev. Lett.* **71** 1641
Camley R E and Barnas J 1989 *Phys. Rev. Lett.* **63** 664
Hsu S Y, Barthelemy A, Holody P, Loloee R, Schroeder P A and Fert A 1997 *Phys. Rev. Lett.* **78** 2652
Borchers J A, Dura J A, Unguris J, Tulchinsky D, Kelley M H, Majkrzak C F, Hsu S Y, Loloee R, Pratt W P Jr and Bass J 1999 *Phys. Rev. Lett.* **82** 2796
[2] Gijs M A M and Bauer G E W 1997 *Adv. Phys.* **46** 285
[3] Ansermet J P 1998 *J. Phys.: Condens. Matter* **10** 6027
[4] Valet T and Fert A 1993 *Phys. Rev.* B **48** 7099
[5] Fert A and Lee S-F 1996 *Phys. Rev.* B **53** 6554
[6] Gehring G A, Gregg J F, Thompson S M and Watson M L 1995 *J. Magn. Magn. Mater.* **140–144** 501
Gregg J F, Allen W, Thompson S M, Watson M L and Gehring G A 1996 *J. Appl. Phys.* **79** 5593
[7] Chiang W-C, Yang Q, Pratt W P Jr, Loloee R and Bass J 1997 *J. Appl. Phys.* **81** 4570
[8] Piraux L, Duboix S, Marchal C, Beuken J M, Filipozzi L, Depres J F, Ounadjela K and Fert A 1996 *J. Magn. Magn. Mater.* **156** 317
[9] Piraux L, Duboix S, Fert A and Belliard L 1998 *Eur. Phys. J.* **4** 413
[10] Gittleman J L, Goldstein Y and Bozowski S 1972 *Phys. Rev.* B **5** 3609

[11] Pratt W P Jr, Lee S F, Slaughter J M, Loloee R, Schroeder P A and Bass J 1991 *Phys. Rev. Lett.* **66** 3060
[12] List N J, Pratt W P Jr, Howson M A, Xu J, Walker M J and Greig D 1995 *J. Magn. Magn. Mater.* **148** 342
[13] List N J, Pratt W P Jr, Howson M A, Xu J, Walker M J, Hickey B J and Greig D 1995 *Mater. Res. Soc. Symp. Proc.* **384** 329
[14] Pratt W P Jr, Lee S F, Holody P, Yang Q, Loloee R, Bass J and Schroeder P A 1993 *J. Magn. Magn. Mater.* **126** 406
[15] Marrows C H and Hickey B J, unpublished
[16] Wiser N 1996 *J. Magn. Magn. Mater.* **159** 119